Supporting information

Tracking *in situ* biodegradation of 1,2-dichloroethenes in a model wetland

Gwenaël Imfeld[a]*, Cristian Estop Aragonés[a], Simone Zeiger[a], Christiane Vitzthum von Eckstädt[b,c], Heidrun Paschke[b], Ralf Trabitzsch[b], Hoger Weiß[b], Hans H. Richnow[a]

Departments of [a]Isotope Biogeochemistry, [b]Groundwater Remediation; Helmholtz Centre for Environmental Research - UFZ, Leipzig D-04318 Germany

[c]Commonwealth Scientific and Industrial Research Organisation-CSIRO, Perth, 6152 Australia (current address)

*Corresponding author:

Gwenaël Imfeld

Department of Isotope Biogeochemistry

Helmholtz Centre for Environmental Research – UFZ

Permoserstr. 15, D-04138 Leipzig, Germany

Phone: +49 (0)341-235-1360

Fax: +49 (0) 341/235-2492

E-mail: gwenael.imfeld@ufz.de

Manuscript for Environmental Science & Technology

Table of content

1. Material and methods

2. 1.1. Detailed scheme of the model constructed wetland and sampling devices

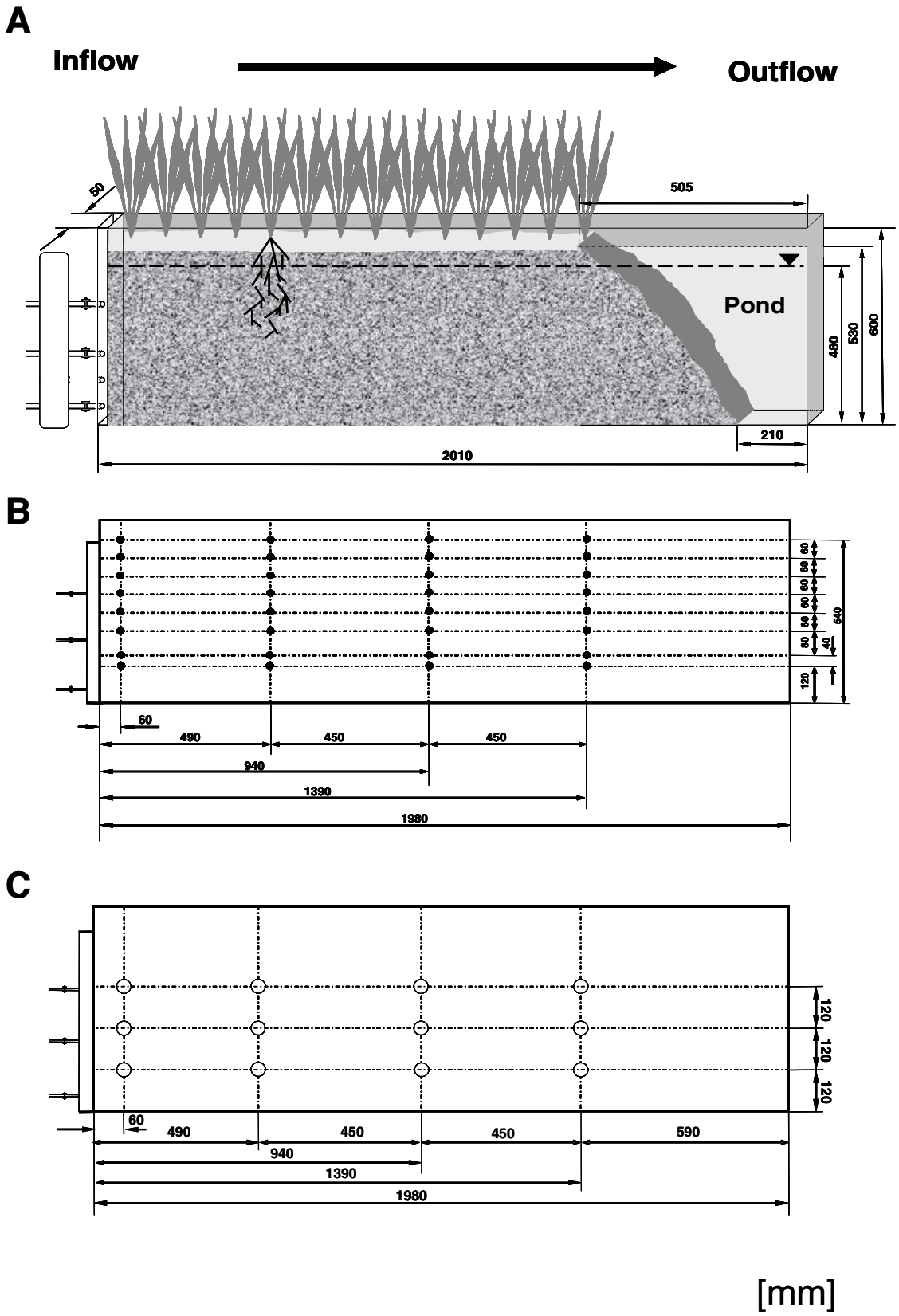

Fig. S1. Detailed scheme of the model constructed wetland (A), locations of the oxygen sensor devices (B) and location of the pore water sampling devices (C). The values are provided in [mm]. The model horizontal subsurface flow wetland consisted of a stainless steel tank (201 x 60 x 5 cm), filled to an average depth of 54 cm with quartz sand ($kf_{average}$ = 2.27 ± 0.14 x 10^{-4} m s^{-1}; grain size = 0.4-0.63 mm) and planted with the common rush (*Juncus effusus*, L.). A 50 cm long water pond at the outflow side remained in direct contact with the atmosphere. The system was equipped with a permanent cooling system maintaining the tank and the wetland at 11°C ± 2 °C. An automatic lighting system simulating day-night irradiation in moderate climates was used in the greenhouse (Wiessner et al., 2005).

(B) A 50 cm long polishing pond at the outflow side remained in direct contact with the atmosphere. The front part of the system consisted of a 1 cm thick glass pane, allowing direct *in situ* oxygen measurements *via* oxygen-sensor devices and direct visual observation of the system. Specific planar oxygen sensor spots (Presens, Regenburg, Germany) attached to the inner part of the glass sealing the system (•), allowed to measure at discrete resolution (Δ ~ 6 cm) dissolved oxygen concentrations in four vertical profiles along the soil compartment (at 6, 49, 94 and 139 cm). Measurements required an oxygen meter device (Fibox 3, Presens, Regenburg, Germany) with fiber-optic oxygen minisensor based on a polymer optical fiber (POF). The device irradiates light through the optical fibber which contacts the glass where the sensor spot is attached (system inner side) causing molecules to excite. Molecules returning to the basic state also irradiate luminescent light which is captured and its intensity is recorded. In the presence of oxygen molecules, excited luminescence molecules can be transferred radiationless to the basic state and the intensity of the luminescence light is diminished. The intensity of the luminescent light is inversely proportional to the oxygen concentration in the sample.

(C) Groundwater was continuously pumped from the 50 L tank and injected at equal flow rate (0.4 mL min^{-1}) by means of three channel pipes (Ø = 4 mm, ISO-VERSINIC®, LIQUID-scan, Überlingen, Germany) before it reached the inflow chamber, passed through the model wetland and is drained away at the pond (175 cm from the inflow). The pump (ICP-N-8,

72 ISMATE, Wertheim-Mondfeld, Germany) was regularly checked during the investigation
73 period. The supplied groundwater in 50 L tanks and maintained under anaerobic conditions at
74 constant N_2 pressure (0.5 mbar). Pore water sampling devices are located at 6, 49, 94, 139 cm
75 from the inflow. At each of these distances, the ports are displayed at 20, 32, and 44 cm depth
76 from the surface (○).

1.2. Quality of the supplied groundwater. The hydrogeochemistry did not substantially vary over time. Overall, the geochemical data of groundwater samples suggested that several terminal electron accepting processes (TEAPs) co-existed over time. The sampled groundwater likely originated from various aerobic and anaerobic sections of the aquifer and the hydrogeochemistry reflected subsurface heterogeneity of biogeochemical reactions. Nitrate (4.5 ± 0.1 mg L^{-1}, *n* = 9) is a potentially relevant electron acceptor. Simultaneously, the presence of ferrous iron (2.3 ± 0.6 mg L^{-1}, ~85% of total iron) suggests microbial iron reduction but it also may have been transported from adjacent zones of the aquifer controlled by other redox reactions. The background concentration of sulphate in the supplied groundwater (747.4 ± 36 mg L^{-1}) was high, but sulphide could not be detected. At the range of redox potential measured (+204 to +478 mV), sulphate reduction is not likely to occur. The main contaminants were *cis*- and *trans*-1,2-DCE, as well as monochlorobenzene with mean concentrations of 1062 ± 63; 284 ± 36 and 810 ± 56 µg L^{-1}, respectively (*n*=9). The overall dominance of the *cis*-DCE isomer over the *trans*- suggests a biological production, as industrial grade DCE usually consists of 60 to 70 % *trans*-DCE (32). Furthermore, concentrations of tetrachlorethene and trichloroethenes were systematically very low (< 5 µg L^{-1}), emphasizing the possible role of reductive dechlorination with concomitant accumulation of DCE as reported elsewhere (27,30). The hydrogeochemical framework was conducive to reductive dechlorination of DCE as suggested by the detection of vinyl chloride (255 ± 98 µg L^{-1}), ethene (21 ± 30 µg L^{-1}) and *Dehalococcoides* spp.-related DNA (data not shown) at favorable pH (6.65 ± 0.19). *Dehalococcoides* sp. related DNA was systematically detected between day 225 and 430 (data not shown). A Dehalococcoides-specific amplification protocol was used for detecting *Dehalococcoides*-affiliated bacteria as previously-described (Hendrickson et al., 2002). However, the simultaneous occurrence of oxidation pathways leading to transient, not detected metabolites can not be excluded.

102 **1.3. Sampling procedure**

103 Pore water samples were retrieved from twelve sampling ports (Fig. 1C) consisting in butyl
104 rubber septa and equipped with stainless steel cannels and nickel-plated luer-lock valves
105 (Roth, Karlsruhe, Germany) across the system at the inflow chamber, and at 6, 49, 94, 139 cm
106 from the inflow. At each of these distances, three depths, 20, 32, and 44 cm from the surface
107 were systematically investigated. In parallel, water samples were collected at the pond (175
108 cm from the inflow). *In situ* oxygen measurements were performed at discrete resolution (Δ = 6
109 cm) through the front glass board in four vertical profiles along the soil compartment at 6, 49,
110 94 and 139 cm from the inflow. During each sampling campaign, aqueous samples were
111 retrieved from sampling ports were systematically dispensed into 20 ml VOC vials for
112 concentration analysis (headspace free), 5 ml vials for geochemical analysis, 20 ml glass vials
113 containing NaCl at saturation point to inhibit further microbial activity (~10 ml headspace) with
114 Teflon-coated septa for isotope composition analysis. Samples were stored on ice and directly
115 transported to the laboratories for chemical analysis and samples for isotope analysis were
116 stored at 4°C until analysis. The same procedure was used for aqueous samples retrieved
117 from the inflow chamber and the pond but 150 ml glass vials containing NaCl at saturation
118 point were used for isotope analysis.
119
120 **1.4. Porewater geochemistry analysis.** Quantification of chlorinated ethenes, ethene and
121 methane was performed with a gas chromatograph equipped with a flame ionisation detector
122 (Varian Chrompack CP-3800, Middelberg, The Netherlands) as previously described. The
123 detection limits of the *cis*-1,2-dichloroethene, *trans*-1,2-dichloroethene, vinyl chloride and
124 ethene were 50, 30, 5 and 5 µg L^{-1}, respectively. Oxygen measurements were performed using
125 a Fibox-3 oxygen meter with fiber-optic oxygen minisensor based on a polymer optical fiber and
126 planar PSt3-oxygen sensors (PreSens, Regenburg, Germany) directly sealed on the inner part
127 of the glass pane. Oxygen concentration was also measured in the tank, inflow and outflow of
128 the model system using colorimetric methods (CHEMets oxygen kits K-7501 and K-7512,
129 CHEMetrics, Düsseldorf, Germany) according to the manufacturer's protocol. Redox potential

and pH were measured on site with the use of a Sen Tix ORP electrode (WTW, Weilheim, Germany) and a Sen Tix 41 (WTW, Weilheim, Germany) electrode, respectively. Nitrite-nitrogen, nitrate-nitrogen, sulphate and chloride anions were analyzed by ion chromatography (DIN EN ISO 10304-2). Photometrical methods were used to determine Fe(II) (DIN 38406-E1), phosphate (DIN EN 1189) and ammonium-nitrogen (DIN 38406-E6) concentrations. Total iron and manganese were analysed by Inductive Coupled Plasma Atomic Emission Spectrometry (ICP-AES) in a CIROS spectrometer (DIN EN ISO 11885). Sulphide concentrations were determined according to the Cline method cline (Cline, 1969). TOC and DOC were analyzed in a Total Organic Carbon analyzer (TOC-5000-500, Shimadzu Europa) and COD was measured by organic matter oxidation with potassium dichromate (Lange cuvette tests, LCK314, Hach Lange LTD, Manchester, UK).

1.5. Compound specific isotope analysis

Stable carbon isotope compositions of chlorinated ethenes were measured using a gas chromatography-combustion-isotope ratio mass spectrometry system (GC-C-IRMS). Aliquots (1000 µL) of head space samples were injected into a gas chromatograph (Agilent 6890; Palo Alto, USA) in split mode connected via a combustion line to a Finnigan MAT 252 isotope ratio mass spectrophotometer via a combustion line. Samples analysis was carried out within 30 days after collection. Samples were heated for at least 1 h at 60°C prior to measurement to enhance partitioning of analytes into the head space and were measured at least in triplicate. Aliquots (500 to 1000 µL) of head space samples were manually injected in a split/splitless injector at 250°C with split ratio set at 1:3. Chromatographic separation was achieved on a CP-PoraBond column (50 m x 0.32 mm ID, 5 µm film; Varian, Palo Alto, USA). The oven temperature program was: 100°C (5 min); 20°C min^{-1} to 150°C; 5°C min^{-1} to 210°C; increase with 20°C min^{-1} to 225°C and hold isotherm for 5 min. The carbon isotope ratio for an individual compound is reported in δ-notation [‰] relative to the Vienna Pee Dee Belemnite standard (V-PDB, IAEA-Vienna) (Eq. 1) (Coplen *et al.*, 2006):

157 $$\delta^{13}C_{compound}\,[\text{‰}] = \left(\frac{(^{13}C/^{12}C)_{\text{compound}}}{(^{13}C/^{12}C)_{\text{Standard}}} - 1 \right) \times 1000\,. \qquad (1)$$

158 The analytical error is ± 0.5 δ unit and incorporates both the accuracy and the reproducibility
159 on replicate measurements of the sample. The relationship between the extent of fractionation
160 and the amount of contaminant degraded is described by the following equation after Mariotti
161 *et al.* (Eq. 2):

162 $$\frac{R}{R_0} = f^{(\alpha-1)} \qquad (2)$$

163 where R is the isotope ratio ($^{13}C/^{12}C$) of the contaminant at a given fraction remaining (f), R_0 is
164 the initial isotope ratio of the contaminant, and α is the estimated fractionation factor for the
165 particular reaction. Estimates of the wetland isotope fractionation factor α were derived from
166 the slope of the standard linear regression plot and converted into an enrichment factors ε
167 according to equation 3:

168 $$\varepsilon[\text{‰}] = (\alpha - 1) \times 1000 \qquad (3)$$

2. Results

2.1. Groundwater and wetland pore water quality.

		Supplied groundwater		Wetland system			
				First period: 0 – 127 [day]		Second period: 199 – 430 [day]	
Variable	***Unit***	***Range***	***Mean (n = 9)***	***Sand compartment (n = 56)***	***Pond (n = 11)***	***Sand compartment (n = 96)***	***Pond (n = 8)***
pH	-	6.2 - 7.0	6.65 ± 0.19[a]	6.81 ± 0.19	7.09 ± 0.11	6.90 ± 0.18[a]	7.26 ± 0.24
Electric conductivity	[mS cm^{-1}]	2.0 - 2.3	2.2 ± 0.1				
Dissolved oxygen	[mg L^{-1}]	2.5 - 5.7	4.7 ± 1	1.59 ± 1.38	> 6[c]	0.40 ± 0.55	3.50 ± 1.50
Redox potential	[mV]	204 - 478	327 ± 71	+173 ± 53	+166 ± 34	-137 ± 155	-52 ± 187
Chloride	[mg L^{-1}]	118 -144	127.1 ± 9	159 ± 32.4	148 ± 23	184 ± 54.6	193 ± 38.3
Sulphate	[mg L^{-1}]	670 - 777	747.4 ± 36	766 ± 104	929 ± 78	741 ± 223	801 ± 327
Nitrate	[mg L^{-1}]	3.3 - 5.8	4.5 ± 1	< LOD	< LOD	< LOD	< LOD
Nitrite	[mg L^{-1}]	< 1.35	< 1.35	n.d.	n.d.	n.d.	n.d.
Sulphide[b]	[µM L^{-1}]	< LOD	< LOD	0.40 ± 1.10	0.90 ± 1.52	366 ± 532	67 ± 125
Iron(II)	[mg L^{-1}]	1.1 - 2.9	2.3 ± 0.6	0.02 ± 0.03	< 0.01	1.72 ± 2.15	1.46 ± 2.38
Tot. iron	[mg L^{-1}]	1.2 - 4.2	2.7 ± 0.9	0.11 ± 0.06	0.09 ± 0.04	3.68 ± 8.90	1.64 ± 2.65
Ammonium	[mg L^{-1}]	n.d.	n.d.	1.59 ± 1.38	0.05 ± 0.03	0.73 ± 0.76	0.55 ± 0.71
Methane	[µg L^{-1}]	n.d.	n.d.	< LOD	< LOD	< LOD	< LOD
Total organic carbon	[mg L^{-1}]	n.d.	n.d.	n.d.	31.6 ± 32.9	n.d.	35.9 ± 33.0
Dissolved organic carbon	[mg L^{-1}]	n.d.	n.d.	n.d.	16.2 ± 11.7	n.d.	33.5 ± 30.2
Dissolved inorganic carbon	[mg L^{-1}]	n.d.	n.d.	n.d.	85.2 ± 15.4	n.d.	96.2 ± 25.8
Chemical oxygen demand	[mg L^{-1}]	n.d.	n.d.	n.d.	18.3 ± 3.7	n.d.	68.9 ± 53.1
Maximal isotope shift ($\Delta\delta^{13}C$)	‰	n.d.	n.d.	*cis*-DCE: 3.8 *trans*-DCE: 2.7	*cis*-DCE: 3.3 *trans*-DCE: 3.6	*cis*-DCE: 28.8 *trans*-DCE: 8.1	*cis*-DCE: 29.3 *trans*-DCE: 7.1
Ethene	[µg L^{-1}]	5.4 - 90.7	20.9 ± 29.4	Refer to body text			
Vinyl chloride	[µg L^{-1}]	202 - 509	255 ± 98				
Trans-1.2-DCE	[µg L^{-1}]	229 - 350	284 ± 36	Average spiked initial concentration 1.5 mg L^{-1}			
1.1-DCE	[µg L^{-1}]	0.2 - 1.2	0.4 ± 0.4	n.d.			
Cis-1.2-DCE	[µg L^{-1}]	1011 - 1218	1062 ± 64	Average spiked initial concentration of 6.5 mg L^{-1}			

Benzene	[µg L^{-1}]	15.4 - 44.0	26.3 ± 10.0	
1.2-Dichloroethane	[µg L^{-1}]	1.4 - 3.2	2.0 ± 0.5	
Trichloroethene	[µg L^{-1}]	1.1 - 4.2	2.5 ± 1.0	n.d.
Tetrachloroethene	[µg L^{-1}]	0.3 - 0.7	0.5 ± 0.1	
Chlorobenzene	[µg L^{-1}]	716 - 871	810 ± 56	

[a]The error range given for the hydrogeochemical variables corresponds to ± σ of the mean value of *n* measurements.

[b]The concentration values of sulphide include S^{-2}, HS^- and H_2S sulphide species.

[c]Colorimetric test only performed at day 127.

< LOD: below limit of detection

n.d.: not determined

Table S1. Selected geochemical variables and contaminants concentration values in groundwater supplied to the constructed wetland and collected at the Bergmannshof contaminated site (Bitterfeld, Germany) and selected geochemical variables concentration values in sand compartment of the model constructed wetland for two phases of the investigation period: day 0 to 127 and day 127 to 430. Values correspond to the investigation period from day 0 to 430. Values for the groundwater quality are provided as the minimal and maximal concentration (range) and the mean values of nine sampling campaigns (*n*=9). Values for the pore water quality of the wetland are provided as the mean values over *n* measurements of measurement values retrieved from each sampling port and at each sampling date.

2.2. Biogeochemical development of the model wetland system

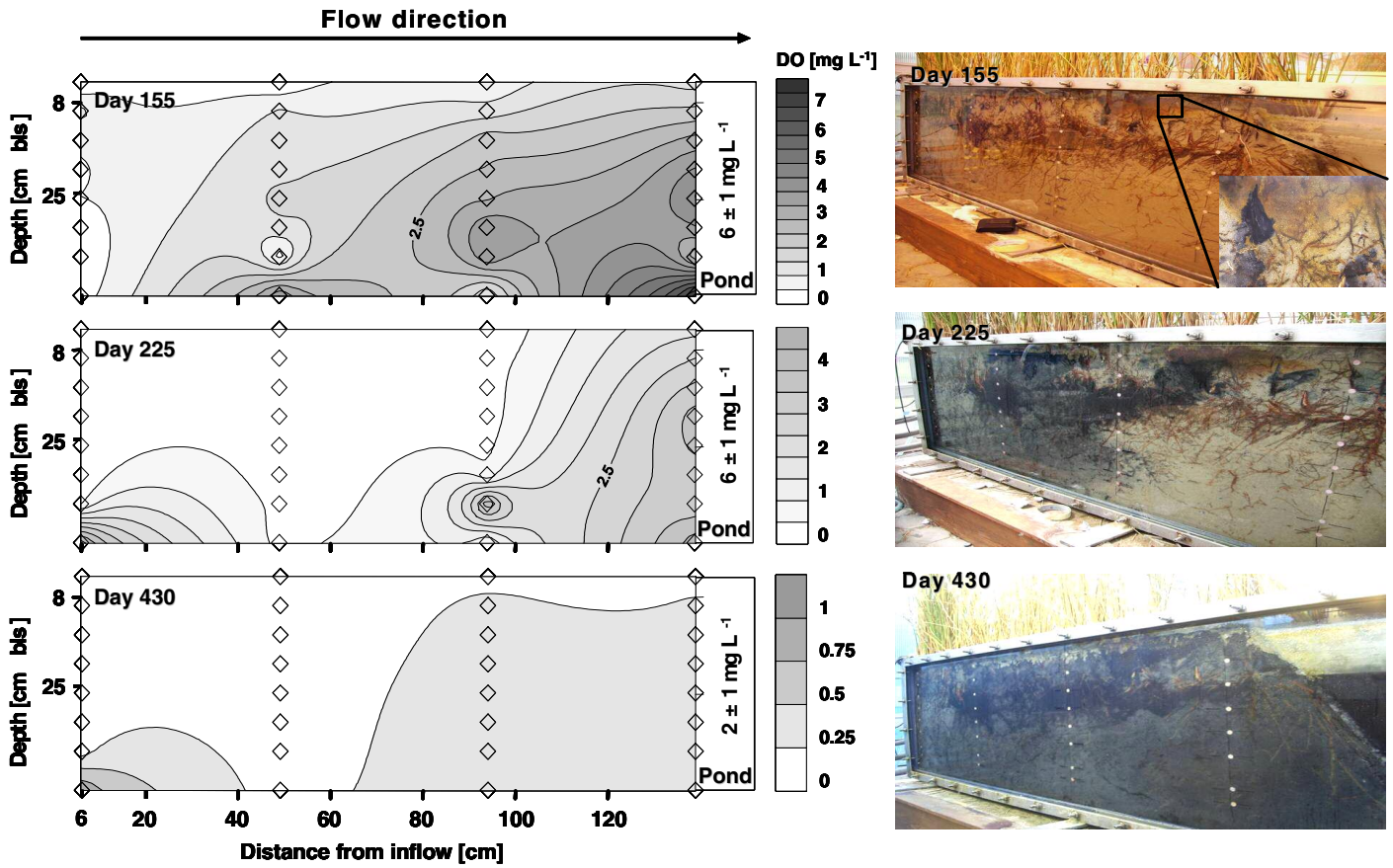

Fig. S2. Spatial and temporal development of oxygen concentrations and iron sulphide minerals precipitation in the model subsurface horizontal-flow model wetland treating *cis*- and *trans*-1,2-dichloroethene (DCE) contaminated groundwater. Oxygen measurements were performed using

205 planar oxygen sensor spots displayed across the system (◊). Distribution of dissolved oxygen concentrations correspond to day 155, 225 and 430
206 and underline the overall trend towards concentration decrease over time. The range of oxygen concentrations changed of one order of
207 magnitude between day 155 (0 to 1 mg L^{-1}) and day 430 (0 to 7 mg L^{-1}). The distribution of oxygen also suggest an overall oxygen concentration
208 decrease with increase depth and a concentration increase over the flow path, indicating the occurrence of spatial gradients of dissolved oxygen.
209 Snapshots of the system taken through the front glass board at different sampling times illustrate the development of major occurring redox
210 processes occurring in the sand compartment. In the unsaturated zone, the formation of reddish-brown iron oxide precipitates at the soil-water-
211 atmosphere interface also occurred in close vicinity of zones where black iron sulphide precipitates were formed (enlarged snapshot at day 155).
212 Since day 199, microbially mediated ferric iron and sulphate reduction processes were detected, which clearly indicates anoxic conditions, as
213 revealed by the geochemical analysis (see above). In this period, precipitates of iron sulphide in the saturated zone of the sand compartment
214 progressively appeared as homogeneous black patches in association or not with the plant rootlets or root. The black front of iron sulphide
215 minerals gradually progressed from the inflow over the flow path since day 200 and reached the sand compartment-pond interface at
216 approximately day 300. This represents an average progression speed of about 1.5 cm day^{-1}. At day 430, anoxic conditions prevail in the whole
217 system and oxygen concentrations were systematically < 0.5 mg L^{-1}.

2.3. Carbon mass balance

Variable	Investigation period [day]					
	0 – 127 (*n* = 10)			199 – 430 (*n* = 8)		
	Inflow [mg L^{-1}]	Outflow [mg L^{-1}]	O/I concentration ratio	Inflow [mg L^{-1}]	Outflow [mg L^{-1}]	O/I concentration ratio
Chemical oxygen demand (COD)	21.5 ± 2.8[a]	18.3 ± 3.7	0.9 ± 0.1	21.4 ± 9.50	68.9 ± 53.1	3.2 ± 8.2
Total organic carbon (TOC)	13.9 ± 8.3	31.6 ± 32.9	2.3 ± 7.4	15.6 ± 24.2	35.9 ± 33.0	2.3 ± 17.1
Dissolved organic carbon (DOC)	8.7 ± 3.8	16.2 ± 11.7	1.9 ± 2.5	15.9 ± 21.8	33.5 ± 30.2	2.1 ± 11.9
Dissolved inorganic carbon (DIC)	72.8 ± 10.4	85.2 ± 15.4	1.2 ± 0.1	58.7 ± 22.7	96.2 ± 25.8	1.6 ± 0.6

[a]The error range given for the hydrogeochemical variables corresponds to ± σ of the mean value of *n* measurements.

Table S3. COD, TOC, DOC and DIC concentrations for wetland inflow and outflow and outflow/inflow concentration ratios for the two investigation period (day 0 to 127 and day 199 to 430). Organic compounds leaching from actively growing plants may be occurring during the first investigation period, whereas leaching from decaying plant and microbial biomass may mainly contribute during the second investigation period.

2.4. *Cis*- and *trans*- DCE removal in the system

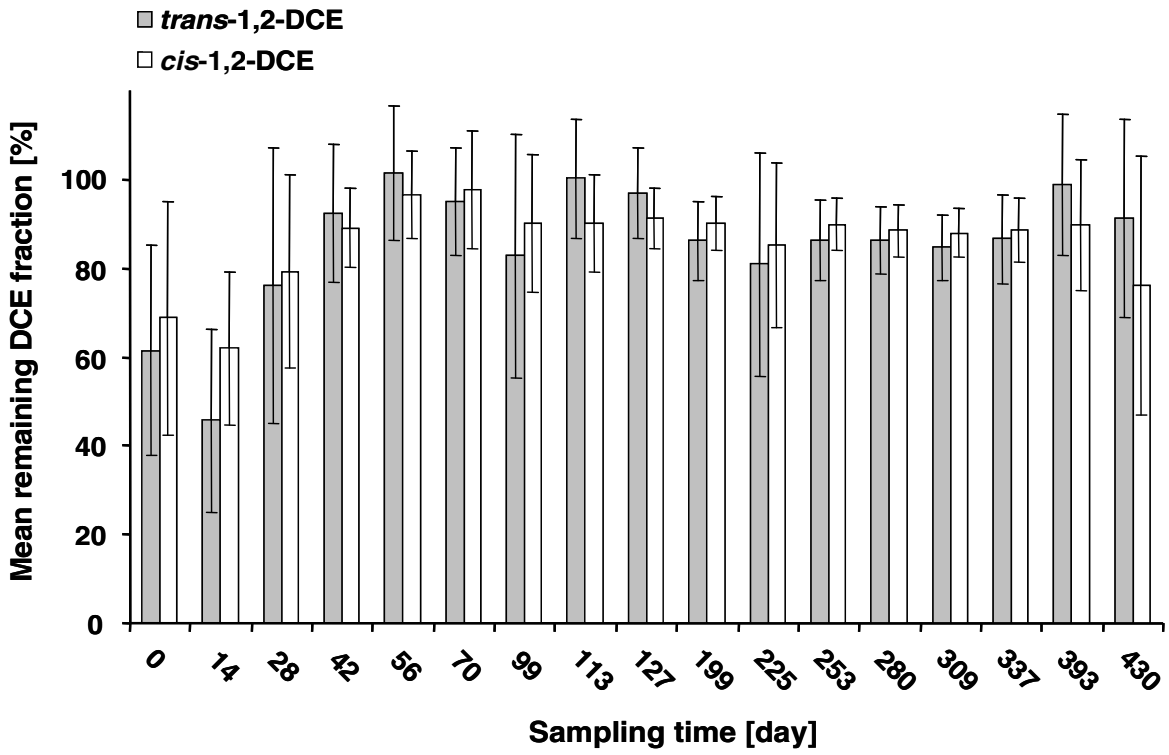

Fig. S3. Mean remaining fraction of *cis*- (white bars) and *trans*-1,2-dichloroethene (grey bars) in the sand compartment over the investigation period. The mean contaminant concentration values were obtained by averaging values obtained from each single sampling port (n=12) across the system and normalized by the initial concentration value at the inflow chamber. The error range given for each normalized value corresponds to the standard deviation and thus indicates the relative spatial variability of the remaining DCE fraction across the wetland.

Distance from inflow [cm below surface]	Depth [cm below surface]	Sampling day					
		176		280		430	
		$\Delta\delta^{13}C$ [‰]	Removed fraction [%]	$\Delta\delta^{13}C$ [‰]	Removed fraction [%]	$\Delta\delta^{13}C$ [‰]	Removed fraction [%]
6	**20**	0	0	0.6	9	1.5	0
49	**20**	0.2	0	1.9	21	6.8	32
94	**20**	0	13	1.8	23	26.4	56
139	**20**	0	0	2.0	13	33.4	61
6	**32**	0.1	0	0.1	5	0	0
49	**32**	0.2	0	1.2	9	3.7	0
94	**32**	0.2	14	1.6	16	13.5	35
139	**32**	0	11	1.9	8	21.7	44
6	**44**	0	0	0	8	0	0
49	**44**	0	0	0.8	5	5.6	5
94	**44**	0	1	2.3	10	16.5	33
139	**44**	0	16	0.7	12	25.6	60

Table. S4. Spatial distribution of the removed *cis*-DCE fraction, (in [%] of the *cis*-DCE concentration at the inflow), and shift in carbon isotopic composition of *cis*-DCE, ($\Delta\delta^{13}C$ [‰], taking the *cis*-DCE isotopic signature at the inflow as a reference) in the model wetland system at representative sampling days (176, 280 and 430). Values correspond to the pore water sampling devices at 6, 49, 94, 139 cm from the inflow. At each of these distances, the ports are displayed at 20, 32, and 44 cm depth from the surface.

2.5. Carbon isotopic enrichment factors

Time	Regression curve		Enrichment factor
[day]	R^2	*p*-value	ε [‰]
0	0.91	0.012	-4.4 ± 0.80[a]
0	0.59	0.131	-2.3 ± 1.14[b]
14	0.92	0.009	-2.0 ± 0.33[a]
14	0.77	0.050	-2.0 ± 0.63[b]
28	0.90	0.013	-1.7 ± 0.33[a]
28	0.70	0.076	-1.8 ± 0.66[b]
42	0.53	0.161	-9.8 ± 5.22[b]
70	0.68	0.087	-2.3 ± 0.92[a]
99	0.56	0.088	-1.2 ± 0.63[a]
199	0.62	0.115	-2.5 ± 1.12[a]
225	0.71	0.073	-2.2 ± 0.83[a]
280	0.85	0.026	-12.2 ± 2.96[a]
280	0.66	0.094	-13.5 ± 5.47[b]
327	0.71	0.073	-13.3 ± 4.82[a]
327	0.77	0.050	-4.0 ± 1.24[b]
393	0.78	0.048	-22.3 ± 6.73[a]
430	0.98	0.001	-32.6 ± 2.30[a]
430	0.84	0.028	-18.8 ± 4.63[b]

Table S5. Mean carbon isotope enrichment factors (ε), coefficient of determination (R^2) and *p*-value of the regression curve for a Rayleigh model for [a]*cis*-1,2-DCE and [b]*trans*-1,2-DCE degradation the constructed wetland over the investigation period (430 days). A single and integrative "mean isotope enrichment factor" was derived for each DCE isomer at each sampling date, taking the inflow chamber values as initial values. For this purpose, discrete-depth concentrations and isotopic composition values retrieved at each of the four vertical profiles across the wetland (6, 49, 94 and 139 cm from the inflow) were separately averaged before a mean enrichment factor was calculated. The enrichment factor was only retrieved if the coefficient of determination was > 0.5. The error range given for the enrichment factor corresponds to the standard error of the predicted y-value in the regression.

Time	Depth below surface	Regression curve		Enrichment factor
[day]	[cm]	R^2	*p*-value	ε [‰]
0	20+32[1]	0.87	0.022	-4.5 ± 2.0[a]
0	44	0.92	0.010	-4.7 ± 0.8[a]
0	44	0.73	0.066	-2.8 ± 1.0[b]
14	20+32[1]	0.82	0.033	-1.7 ± 0.4[a]
14	44	0.97	0.002	-2.6 ± 0.3[a]
14	20+32[1]	0.72	0.069	-1.8 ± 0.6[b]
14	44	0.93	0.008	-2.7 ± 0.4[b]
28	20+32[1]	0.80	0.041	-1.7 ± 0.5[a]
28	44	0.83	0.032	-1.9 ± 0.5[a]
28	44	0.81	0.038	-1.5 ± 0.4[b]
42	44	0.75	0.057	-8.9 ± 2.9[b]
56	44	0.72	0.068	-6.7 ± 2.4[a]
225	20	0.81	0.036	-3.7 ± 0.3[a]
225	44	0.83	0.031	-5.2 ± 0.4[a]
280	20	0.74	0.060	-7.6 ± 0.6[a]
337	20	0.86	0.023	-7.8 ± 0.5[a]
337	32	0.89	0.017	-16.6 ± 0.5[a]
393	20	0.77	0.050	-18.0 ± 2.3[a]
393	32	0.72	0.069	-22.1 ± 2.1[a]
430	20	0.94	0.006	-33.7 ± 4.4[a]
430	32	0.96	0.004	-31.4 ± 2.3[a]
430	44	0.96	0.004	-27.2 ± 2.7[a]

Table S6. Carbon isotope enrichment factors (ε), coefficient of determination (R^2) and *p*-value of the regression curve corresponding to a Rayleigh model for [a]*cis*-1,2-DCE and [b]*trans*-1,2-DCE degradation the constructed wetland over the investigation period (430 days). Raw data were obtained from porewater samples retrieved across the wetland along the flow path at three distinct depths: 20 cm, 32 cm and 44 cm. Isotope composition and concentration data were also evaluated separately for each investigated depths. Three enrichment factors were then retrieved for each specific flow path per sampling date and per DCE isomer, taking the inflow chamber values as initial values. An enrichment factor was only retrieved if the coefficient of determination was > 0.5. [1]Equally pooled samples corresponding to samples from depths 20 and 32 cm below the surface level. The error range given for the enrichment factors correspond to the standard error of the predicted y-value in the regression.

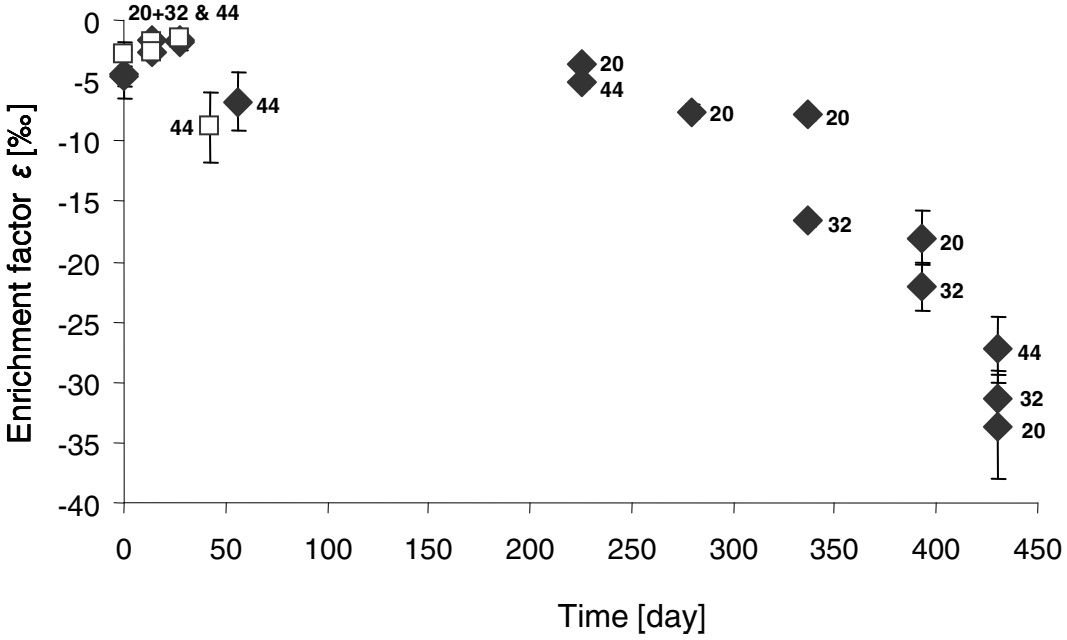

Fig. S4. Temporal changes in carbon enrichment factors of *cis*-1,2-DCE (♦) and *trans*-1,2-DCE (□) obtained by fitting a Rayleigh model to concentration and isotope composition data. The enrichment factors correspond to mean data retrieved from a single flow path across the wetland at 20, 32 and 44 cm depth below the surface. Numbers associated with the symbols indicate the depth of the flow path on which the enrichment factor was retrieved. For all the enrichment factors, coefficient of determination (R^2) of the linear regression curve of the respective Rayleigh model was > 0.5.

344 **3. Literature Cited**

345 Cichocka D.; Imfeld G.; Richnow H.H.; I., N., High variability of stable carbon isotope
346 fractionation upon microbial reductive dechlorination of tetra- and trichloroethene.
347 Chemosphere 2008, 71, 639-648.

348 Cline, J.D., Spectrophotometric Determination of Hydrogen Sulphide in Natural Waters.
349 Limnology and Oceanography 1969, 14, 454-&.

350 Coplen, T.B., Brand, W.A., Gehre, M., Groning, M., Meijer, H.A., Toman, B., Verkouteren, RM.,
351 After two decades a second anchor for the VPDB delta ^{13}C scale. Rapid Commun Mass Sp.
352 2006, 20, 3165-3166.

353 Hendrickson, E.; Payne, J.; Young, R.; Starr, M.; Perry, M.; Fahnestock, S.; Ellis, D.; Ebersole,
354 R., Molecular analysis of Dehalococcoides 16S ribosomal DNA from chloroethene-
355 contaminated sites throughout north America and Europe. Applied and Environmental
356 Microbiol. 2002, 68, 485-495.

357 Mariotti, A., Denitrification in Groundwaters, Principles and Methods for Its Identification - a
358 Review. J. Hydrol. 1986, 88, 1-23.

359 Wiessner, A.; Kappelmeyer, U.; Kuschk, P.; Kastner, M., Influence of the redox condition
360 dynamics on the removal efficiency of a laboratory-scale constructed wetland. Water Res.
361 2005, 39, 248-256.